

# A proposed agglomerate model for oxygen reduction in the catalyst layer of proton exchange membrane fuel cells

Zhang, Xiaoxian; Gao, Yuan; Ostadi, Hossein; Jiang, Kyle; Chen, Rui

DOI:

[10.1016/j.electacta.2014.10.127](https://doi.org/10.1016/j.electacta.2014.10.127)

License:

Other (please specify with Rights Statement)

Document Version

Peer reviewed version

Citation for published version (Harvard):

Zhang, X, Gao, Y, Ostadi, H, Jiang, K & Chen, R 2014, 'A proposed agglomerate model for oxygen reduction in the catalyst layer of proton exchange membrane fuel cells', *Electrochimica Acta*, vol. 150, pp. 320-328. <https://doi.org/10.1016/j.electacta.2014.10.127>

[Link to publication on Research at Birmingham portal](#)

## Publisher Rights Statement:

NOTICE: this is the author's version of a work that was accepted for publication in *Electrochimica Acta*. Changes resulting from the publishing process, such as peer review, editing, corrections, structural formatting, and other quality control mechanisms may not be reflected in this document. Changes may have been made to this work since it was submitted for publication. A definitive version was subsequently published in *Electrochimica Acta*, Vol 150, December 2014, DOI: 10.1016/j.electacta.2014.10.127.

Eligibility for repository checked March 2015

## General rights

Unless a licence is specified above, all rights (including copyright and moral rights) in this document are retained by the authors and/or the copyright holders. The express permission of the copyright holder must be obtained for any use of this material other than for purposes permitted by law.

- Users may freely distribute the URL that is used to identify this publication.
- Users may download and/or print one copy of the publication from the University of Birmingham research portal for the purpose of private study or non-commercial research.
- User may use extracts from the document in line with the concept of 'fair dealing' under the Copyright, Designs and Patents Act 1988 (?)
- Users may not further distribute the material nor use it for the purposes of commercial gain.

Where a licence is displayed above, please note the terms and conditions of the licence govern your use of this document.

When citing, please reference the published version.

## Take down policy

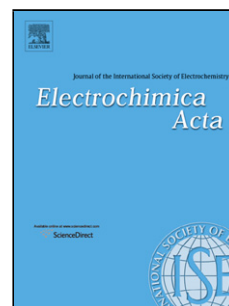
While the University of Birmingham exercises care and attention in making items available there are rare occasions when an item has been uploaded in error or has been deemed to be commercially or otherwise sensitive.

If you believe that this is the case for this document, please contact [UBIRA@lists.bham.ac.uk](mailto:UBIRA@lists.bham.ac.uk) providing details and we will remove access to the work immediately and investigate.

## Accepted Manuscript

Title: A proposed agglomerate model for oxygen reduction in the catalyst layer of proton exchange membrane fuel cells

Author: Xiaoxian Zhang Yuan Gao Hossein Ostadi Kyle Jiang Rui Chen



PII: S0013-4686(14)02135-5  
DOI: <http://dx.doi.org/doi:10.1016/j.electacta.2014.10.127>  
Reference: EA 23643

To appear in: *Electrochimica Acta*

Received date: 3-10-2014  
Revised date: 24-10-2014  
Accepted date: 26-10-2014

Please cite this article as: Xiaoxian Zhang, Yuan Gao, Hossein Ostadi, Kyle Jiang, Rui Chen, A proposed agglomerate model for oxygen reduction in the catalyst layer of proton exchange membrane fuel cells, *Electrochimica Acta* <http://dx.doi.org/10.1016/j.electacta.2014.10.127>

This is a PDF file of an unedited manuscript that has been accepted for publication. As a service to our customers we are providing this early version of the manuscript. The manuscript will undergo copyediting, typesetting, and review of the resulting proof before it is published in its final form. Please note that during the production process errors may be discovered which could affect the content, and all legal disclaimers that apply to the journal pertain.

## Aproposed agglomerate model for oxygen reduction in the catalyst layer of proton exchange membrane fuel cells

Xiaoxian Zhang<sup>a</sup>, Yuan Gao<sup>b</sup>, Hossein Ostadi<sup>c</sup>, Kyle Jiang<sup>d</sup>, Rui Chen<sup>e</sup>

<sup>a</sup> School of Engineering, University of Liverpool, Brownlow Street, Liverpool, L69 3GQ UK. e-mail: [Xiaoxian.zhang@liverpool.ac.uk](mailto:Xiaoxian.zhang@liverpool.ac.uk)

<sup>b</sup> Clean Energy Automotive Engineering Centre & School of Automotive Studies, Tongji University, Shanghai 201804, China e-mail: [yuangao@tongji.edu.cn](mailto:yuangao@tongji.edu.cn)

<sup>c</sup> Intelligent Energy, Charnwood Building, Holywell park, Loughborough, Leicestershire, LE11 3GB, UK. e-mail: [Hossein.Ostadi@intelligent-energy.com](mailto:Hossein.Ostadi@intelligent-energy.com)

<sup>d</sup> School of Mechanical and Engineering, University of Birmingham, Birmingham B15 2TT, UK. e-mail: [k.jiang@contacts.bham.ac.uk](mailto:k.jiang@contacts.bham.ac.uk)

<sup>e</sup> Department of Aeronautical and Automotive Engineering, Loughborough University, Leicestershire LE11 3TU, UK. e-mail: [R.Chen@lboro.ac.uk](mailto:R.Chen@lboro.ac.uk)

### The highlights:

- We developed a new agglomerate model to describe oxygen reduction reaction.
- We showed how to calculate the model parameters from catalyst layer structure.
- We verified the agglomerate model.

### Abstract

Oxygen diffusion and reduction in the catalyst layer of PEM fuel cell is an important process in fuel cell modelling, but models able to link the reduction rate to catalyst-layer structure are lack; this paper makes such an effort. We first link the average reduction rate over the agglomerate within a catalyst layer to a probability that an oxygen molecule, which is initially on the agglomerate surface, will enter and remain in the agglomerate at anytime in the absence of any electrochemical reaction. We then propose a method to directly calculate distribution function of this probability and apply it to two catalyst layers with contrasting structures. A formula is proposed to describe these calculated distribution functions, from which the agglomerate model is derived. The model has two parameters and both can be independently calculated from catalyst layer structures. We verify the model by first showing that it is an improvement and able to reproduce what the spherical model describes, and then testing it against the average oxygen reduction directly calculated from pore-scale simulations of oxygen diffusion and reaction in the two catalyst layers. The proposed model is simple, but significant as it links the average oxygen reduction to catalyst layer structures, and its two parameters can be directly calculated rather than by calibration.

**Key words:** PEM fuel cells; catalyst layer; agglomerate model; pore-scale simulations.

**Nomenclature**

$c$	concentration of dissolved oxygen within agglomerates
$c_{im}$	volumetric average of $c$ over the agglomerates
$c_m$	average dissolved oxygen concentration on the outer surface of agglomerates
	gaseous oxygen concentration in the inter-agglomerate pores dissolved
$C$	oxygen concentration in ionomer in equilibrium with $C$
$C^{eq}$	
$c_{ref}$	reference dissolved oxygen concentration
$D$	effective diffusion coefficient of the intra-agglomerate pores for gaseous oxygen
$D_0$	diffusion coefficient of ionomer for dissolved oxygen
$D_{eff}$	effective diffusion coefficient of inter-agglomerate pores for dissolved oxygen
	effectiveness factor in the absence of ionomer film
$E$	effectiveness factor in the presence of ionomer film
$E'$	
$F$	Faraday constant
$i_{ref}$	reference exchange current density
$k_c$	oxygen reduction rate
$M(t)$	mass of dissolved oxygen in agglomerates at time $t$
$r_{gg}$	radius of spherical agglomerates
$r(t)$	increasing rate of dissolved oxygen in agglomerates at time $t$
$R$	gas constant
$R_0$	consumption rate of gaseous oxygen in inter-agglomerate pores
$R_e$	average oxygen reduction rate in the agglomerates
$S_a$	volumetric reactive surface area of the catalyst in agglomerates
$S_0$	specific outer surface area of agglomerates
$T$	temperature
$V_i$	volume of each voxel in the 3D image of the catalyst layer
$v_i$	average volume of ionomer in each agglomerate voxel
$\alpha$	mass exchange rate coefficient between oxygen in intra-agglomerate and inter-agglomerate pores.
$\alpha_c$	cathodic transfer coefficient
$\beta$	equilibrium constant between gaseous oxygen and oxygen dissolved in ionomer
$\eta$	overpotential

$\theta_{im}$	volumetric ionomer content in the intra-agglomerate pores
$\theta_m$	inter-agglomerate porosity
$\alpha$	agglomerate model parameter
$\kappa$	agglomerate model parameter
$\varepsilon$	size of voxel in the 3D images
$\lambda$	thickness of the ionomer film

ACCEPTED MANUSCRIPT

## 1. Introduction

Platinum supported by carbon grains is often used as the catalyst in proton exchange membrane (PEM) fuel cell[1]. The carbon grains are further bound by an ionomer to make the catalyst layer[2]. In manufacturing, the grain particles tend to aggregate, forming agglomerates with the nanopores (intra-agglomerate pores) inside them much smaller than the pores (inter-agglomerate pores) between them. In the cathode, gaseous oxygen moves into the inter-agglomerate pores first from the gas diffusion layer, and then diffuses into the agglomerates where it reacts with proton and electron, in the presence of the catalyst, to form water[3]. The catalyst layer has a bi-mode pore structure, but these pores cannot be explicitly resolved in fuel cell modelling. Instead, their impacts on oxygen diffusion and reaction are described by volumetric average parameters: effective diffusion coefficient for gaseous oxygen diffusion in the inter-agglomerate pores and agglomerate model for oxygen diffusion and reaction inside the agglomerates[4, 5].

The agglomerates in catalyst layers are geometrically complicated [6, 7]. In earlier fuel cell modelling, oxygen diffusion through the pores inside the agglomerates was assumed to be fast and the potential loss due to it was often neglected[8]. This assumption is only rationale at low overpotential, in which the electrochemical reaction rate is slow and oxygen diffusion through the agglomerates is comparably fast. As a result, oxygen distribution within the agglomerates is relatively uniform and its accessibility to all catalyst particles inside the agglomerates is almost the same. When a cell works at high overpotential, however, the electrochemical rate is comparable to the maximum oxygen diffusion rate. This would create a concentration gradient, in which the catalysts in the proximity of the agglomerate surfaces have a better accessibility to oxygen than the catalyst in other areas. Therefore, the efficiency of the catalysts reduces, and oxygen diffusion becomes a limiting factor [9]. How to describe the impact of such oxygen-diffusion limitation on electrochemical reaction is essential to

help catalyst layer design, and has attracted increased attention over the past few years [10, 11].

The models that aim to describe the decrease in electrochemical reaction due to oxygen-diffusion limitations are known as agglomerate model in the literature. Apparently, the only available agglomerate model is the so-called spherical agglomerate model [12]. The assumption of the spherical model is that the agglomerates in the catalyst layer are non-touched spheres with the same diameter. Real agglomerates, however, are more geometrically complicated and approximating them by a number of non-touched spheres with a single diameter is an obvious oversimplification [13, 14]. Since oxygen reaction in the catalyst layer depends on oxygen diffusion from the inter-agglomerate pores into the intra-agglomerate pores, which in turn depends on the agglomerate geometry, the spherical model is inadequate to describe oxygen reduction when oxygen diffusion becomes a limiting factor. In fact, recent work has shown that when approximating the oxygen reaction in a given catalyst layer using the spherical model, its agglomerate diameter is just a fitting parameter rather than a geometrical description of the agglomerates; the value of its agglomerate diameter needs to change with overpotential in order to correctly describe the average reaction rate [15, 16].

The average oxygen reaction in a catalyst layer depends on its geometry and oxygen diffusion in its agglomerates. Because the oxygen diffusion and reaction are difficult to measure, pore-scale modelling and tomography have been used increasingly in the past few years to bridge this gap [17, 18]. For example, using X-ray tomography or focused ion beam/scanning electron microscopy (FIB/SEM) tomography, one can visualise the interior structures of a catalyst layer at resolutions as fine as a few nanometres [7, 19]. These, together with the development in computational physics, have substantially improved our understanding of some fundamental transport and reaction processes in the catalyst layer,



which would remain unknown otherwise[20-22]. There has been a surge in use of tomography and pore-scale model over the past few years to visualise and simulate catalyst layers[23]. For a catalyst layer with its 3D structure acquired by tomography, one can numerically calculate the average oxygen reduction rate within it under different operating conditions and then save the results in tabular forms as an input database for fuel cell modelling[15]. This database, however, could become extremely huge and time-consuming to obtain if a variety of operating conditions need to be considered. Therefore, it is practically useful if we can find a simple formula to represent this database.

The purpose of this paper is to present such a formula. To derive the formula, we first establish the link between the average oxygen reaction rate and a probability that an oxygen molecule, which is initially on the agglomerate surfaces, enters and then remains in the agglomerates at any time in the absence of any electrochemical reactions. We explain how to directly calculate the distribution function of this probability based on pore-scale simulation of oxygen diffusion, and then apply it to two catalyst layers with contrasting structures. The first one is an idealised catalyst layer packed by overlapped spheres, and the second one is a real catalyst layer acquired using FIB/SEM tomography. A formula is proposed to describe the distribution function of this probability calculated from the two samples, from which an agglomerate model is analytically derived. We verify the model by first showing that it is an improvement and can produce all the spherical agglomerate model can describe, and then testing it against the average electrochemical reaction rates directly calculated from pore-scale simulations of oxygen diffusion and reaction in the two catalyst layers under different overpotentials

## 2. Background and theory

Practical fuel cell modelling focuses on large scale and cannot explicitly resolve the individual pores within the catalyst layer where the electrochemical reaction takes place. In

these models, all processes occurring at the pore scales are volumetrically averaged. In averaging the catalyst layer, the impact of the inter-agglomerate porosity is represented by an effective diffusion coefficient, and the impact of the intra-agglomerate pores and catalyst loading are described by an agglomerate model [10, 24]. In macroscopic fuel cell modelling, the combination of gaseous oxygen diffusion in the inter-agglomerate pores and oxygen diffusion and reduction in the intra-agglomerate pores are described by

$$\frac{\partial \theta_m C}{\partial t} = \theta_m D \nabla^2 C + R_0, \quad (1)$$

where  $C$  is the gaseous oxygen concentration in the inter-agglomerate pores,  $\theta_m$  is inter-agglomerate porosity,  $D$  is the effective diffusion coefficient of the inter-agglomerate pores for gaseous oxygen, and  $R_0$  is the dissolving rate of the gaseous oxygen into ionomer and liquid water on the outer surface of the agglomerates. When the reaction in a fuel cell is in steady state, the dissolving rate  $R_0$  is the same as the electrochemical reaction rate. Prior to reaching a steady state, however, only part of  $R_0$  is consumed by electrochemical reaction and the remaining part leads to an increase in oxygen concentration in the agglomerates. The value of  $R_0$  depends on catalyst loading, agglomerate geometry and oxygen diffusion in the intra-agglomerates, and we will discuss how to find this dependence in the following sections.

## 2.1. Oxygen diffusion in agglomerates and a simple agglomerate model

The movement of gaseous oxygen from the inter-agglomerate pores into the agglomerates is often modelled as a diffusion process. The gaseous oxygen, however, needs to dissolve in the ionomer on the outer surface of the agglomerates first before diffusing into the agglomerates as the agglomerates are normally assumed to be fully filled by the ionomer. Figure 1 shows a cross-section of a typical catalyst layer. If the oxygen concentration inside the agglomerates does not change considerably over space and can be approximated by an average concentration  $c_{im}$ , a simple approach to describe the transfer rate

of the oxygen from the agglomerate surfaces into the agglomerates is to assume that this rate is proportional to the difference between the dissolved oxygen concentration on the agglomerate surfaces,  $c_m$ , and a representative concentration inside the agglomerates,  $c_{im}$ .

Before the system reaches steady state, part of this transfer rate is used to sustain the electrochemical reaction, and the remaining part leads to an increase in oxygen concentration within the agglomerates. Their relationships can be described by the following mass-balance equation:

$$R_0 = \alpha \theta_{im} (c_m - c_{im}) = \frac{\partial(\theta_{im} c_{im})}{\partial t} + k_c \theta_{im} c_{im}, \quad (2)$$

where  $\alpha$  is a transfer rate coefficient,  $\theta_{im}$  is the volumetric ionomer content in the agglomerates. The relationship between the gaseous oxygen concentration  $C$  and the dissolved oxygen concentration in the ionomer on the agglomerate surface is described by the Henry' law,  $c_m = \beta C$ . The transfer rate coefficient depends on the average size  $\gamma$  and the effective diffusion coefficient  $D_{eff}$  of the agglomerates; we can express this dependence as  $\alpha = \chi D_{eff} / \gamma^2$  where  $\chi$  is a parameter. As proven in the appendix, Eq.(2) can be rewritten as follows as a function of  $c_m$  only:

$$\frac{\partial c_{im}}{\partial t} + k_c c_{im} = \int_0^t \frac{\partial c_m}{\partial \tau} g(t-\tau) e^{-k_c(t-\tau)} d\tau + k_c \int_0^t c_m(\tau) g(t-\tau) e^{-k_c(t-\tau)} d\tau \quad (3)$$

where  $g(t) = \alpha \exp(-\alpha t)$  is a probability distribution function. Substituting Eq. (3) into Eq. (1) yields

$$\frac{\partial \theta_m C}{\partial t} = \theta_m D \nabla^2 C - \int_0^t \frac{\partial c_m}{\partial \tau} g(t-\tau) e^{-k_c(t-\tau)} d\tau - k_c \int_0^t c_m(\tau) g(t-\tau) e^{-k_c(t-\tau)} d\tau. \quad (4)$$

The diffusion and reaction are assumed to have reached a steady state at  $t \rightarrow \infty$ . At steady state, the second term on the right-hand side of Eq.(4) is zero, and the third term describes the average reaction rate at steady state. That is,

$$\begin{aligned}
R_e &= \alpha k_c \int_0^\infty c_m \exp[-(\alpha + k_c)\tau] d\tau \\
&= \frac{k_c c_m}{1 + k_c / \alpha} = E k_c c_m
\end{aligned} \quad (5)$$

where the parameter  $E = 1/(1 + k_c / \alpha)$  is the effectiveness factor, describing the decreased reaction rate due to diffusion limitation. If the diffusion coefficient of the agglomerates is relatively large or the agglomerate sizes are relatively small such that  $\alpha = \chi D_{eff} / \gamma^2 \gg k_c$ ,  $E \approx 1$  and oxygen diffusion in the agglomerates is not a limiting factor. In PEM fuel cell, the oxygen reaction rate inside the agglomerates is often described by the Butler-Volmer equation:

$$k_c = \frac{S_a i_{ref}}{4 F c_{ref}} \left[ \exp\left(\frac{\alpha_c F}{RT} \eta\right) - \exp\left(-\frac{(1 - \alpha_c) F}{RT} \eta\right) \right]. \quad (6)$$

where  $S_a$  is the electrochemically active surface area of the catalyst in a unit volume of the agglomerates,  $F$  is Faraday constant,  $i_{ref}$  is reference exchange current density,  $c_{ref}$  is reference oxygen concentration,  $\alpha_c$  is cathode transfer coefficient,  $T$  is temperature,  $R$  is gas constant, and  $\eta$  is overpotential - the difference between the potentials of protons and electrons.

If the agglomerates in a catalyst layer are non-touched spheres with a single diameter, the decrease of oxygen reaction due to the diffusion limitation in the spheres can be described by the following spherical agglomerate model[25]:

$$\begin{aligned}
R_e &= E k_c c_m, \\
E &= \frac{1}{\Phi} \left( \frac{1}{\tanh(3\Phi)} - \frac{1}{3\Phi} \right), \quad (7) \\
\Phi &= \frac{1}{3} \sqrt{\frac{r_{agg}^2 k_c}{D_{eff}}},
\end{aligned}$$

where  $r_{agg}$  is the radius of the sphere.

The spherical model considers the spatial variation of the oxygen concentration within the sphere, whilst the simple model uses a representative concentration to describe the impact of this spatially varying oxygen concentration in the sphere on the average oxygen reduction rate. It is hence interesting to compare the behaviours of the simple and the spherical models. For ease of analysis, in what follows, we normalised the parameters in front of the square bracket on the right-hand side of Eq.(6) as follows:

$$k_0 = \frac{r_{agg}^2 S_a i_{ref}}{D_{eff} 4F c_{ref}} \quad (8)$$

We assumed that the diameter of the spheres is 300nm and its effective diffusion coefficient for oxygen is  $138.8 \mu\text{m}^2/\text{s}$ . In comparison of the two models, the value of parameter  $\chi$  in the simple model was chosen such that the solutions of the two models cross at  $E=0.5$ . The final result is  $\chi = 24$ , meaning that the transfer rate coefficient in the simple model is  $\alpha=0.036\text{s}^{-1}$ .

Figure 2 compares the effectiveness factors calculated by the two models under different overpotentials. There is a slight difference between them, but their decays with overpotential are comparable. In comparison with the spherical model, the simple model underestimates the efficiency at low overpotential and overestimates it at high overpotential.

The above example aimed to introduce an alternative way to model oxygen reduction in the catalyst layer rather than to demonstrate which model is superior. Because the spherical agglomerate model assumed that the agglomerates in the catalyst layer are non-touched spheres with a single diameter, it is inadequate to describe the electrochemical reaction rate when oxygen diffusion becomes a limiting factor. In fact, recent work has found that for a given catalyst layer, the agglomerate diameter in the spherical model is just a fitting parameter, and its value is not a constant but changes with overpotential [15, 16]. That is, in using the spherical model, the value of its agglomerate diameter estimated from one overpotential is inaccurate to calculate the reaction rates under other overpotentials.

## 2.2. Relationship between agglomerate model and memory function

The function  $g(t) = \alpha \exp(-\alpha t)$  in Eq. (3) was derived by assuming that the oxygen transfer rate from the inter-agglomerate pores into the agglomerates is proportional to the difference between the oxygen concentration on the outer surface of the agglomerate and a representative oxygen concentration within the agglomerates. Physically,  $g(t)$ , known as memory function in the literature, is the probability that an inert molecule, which is initially on the agglomerate surfaces, enters and stays in the agglomerates at time  $t$  [26, 27]. Eqs. (4) and (5) assume this probability is exponential, which, as will be demonstrated later, is just an approximation and inaccurate. If we can find an improved function to accurately describe this probability for most catalyst layers, we should be able to improve the agglomerate model.

For a given catalyst layer, we can design a specific scenario to calculate its memory function  $g(t)$ . For doing so, we set the initial oxygen concentration inside the agglomerates to be zero, and the gaseous oxygen concentration in the inter-agglomerate pores to increase from zero to  $C$  and then remain unchanged. Since the gaseous oxygen needs to dissolve into the ionomer first before it can move into the agglomerate, the dissolved oxygen concentration on the agglomerate surfaces can be calculated from the Henry law of  $C^{eq} = \beta C$ . Mathematically, this change can be described by  $\partial c_m / \partial t = C^{eq} \delta(0)$  where  $\delta(0)$  is the delta function. Under these specific initial and boundary conditions, the gaseous oxygen concentration gradient in the inter-agglomerate pores is zero, and the first term on the right-hand side of Eq. (4) is zero. If we make the electrochemical reaction be zero, i.e.,  $k_c = 0$ , Eq. (3) reduces to

$$\frac{1}{C^{eq}} \frac{\partial c_{im}}{\partial t} = g(t). \quad (9)$$

Eq. (9) reveals that under the above initial and boundary conditions, the memory function  $g(t)$  at time  $t$  is equivalent to the normalised increasing rate of the oxygen mass in the agglomerates in the absence of reactions. From Eq. (3), the agglomerate model is the second

term on its right-hand side when  $t \rightarrow \infty$ . Therefore, once the memory function is known, the oxygen reduction rate can be derived from

$$R_e = k_c \int_0^{\infty} g(\tau) e^{-k_c \tau} d\tau, \quad (10)$$

In what follows, we will demonstrate how to directly calculate the memory function based on pore-scale simulations of oxygen diffusion in two catalyst layers with contrasting structures.

### 3. Calculate the memory function

Figure 3 shows the two catalyst layers we investigated. The first one is an idealised catalyst layer packed by non-overlapped spheres [28], and the second one is a real catalyst layer acquired using FIB/SEM tomography [15]. Due to computer power, for each catalyst layer we only used half of the original image shown in Figure 3 for simulations. The memory function of each sample was calculated from pore-scale simulations under the conditions that lead to Eq.(9). In the two images shown in Figure 3, diffusion and reaction of the dissolved oxygen in their agglomerates were described by the following equation:

$$\frac{\partial c}{\partial t} = D_{eff} \nabla^2 c - k_c c, \quad (11)$$

where  $c$  is the concentration of the dissolved oxygen in the ionomer within the agglomerates,  $D_{eff}$  is the effective diffusion coefficient of the agglomerates. The boundary conditions for Eq.(11) are the interface between the inter-agglomerate pores, which is made transparent in Figure 3, and the agglomerates shown in Figure 3. For ease of analysis, we normalised the time, space and concentration as follows in all simulations

$$\begin{aligned}
\frac{\partial c'}{\partial t'} &= \nabla^2 c' - k'_c c', \\
c' &= c / C^{eq}, \\
t' &= D_{eff} t / \varepsilon^2, \\
\mathbf{x}' &= \mathbf{x} / \varepsilon, \\
k'_c &= k_0 \left[ \exp\left(\frac{\alpha_c \eta F}{RT}\right) - \exp\left(\frac{(1-\alpha_c) \eta F}{RT}\right) \right], \\
k_0 &= \frac{\varepsilon^2 S_a i_{ref}}{D_{eff} 4F c_{ref}}.
\end{aligned} \tag{12}$$

where  $\varepsilon$  is the side-length of the voxels in the 3D images. For convenience of presentation, in what follows we will drop the prime associated with the normalised variables.

To be consistent with the ways the agglomerate model has been used in the literature, the overpotential across each of the simulated images was assumed to be a constant. This can be justified as the size of the images is just two microns. In all simulations, the initial oxygen concentration in the agglomerates was zero, and the normalised concentration of the dissolved oxygen on the outer surface of the agglomerates was 1.0. For calculating the memory function, we set  $k_0 = 0$ , that is, there is no electrochemical reaction.

Oxygen diffusion through the agglomerates in each image was simulated using a model we developed previously for pore-scale simulation of water flow and chemical transport in soils and rocks [29]. As an example to illustrate how the catalyst structures affect oxygen diffusion, Figure 4 shows the simulated concentration snapshots at time  $t' = 15$  for the two images.

In each simulation, the oxygen concentrations in all voxels were sampled after each time step, which were used to calculate the oxygen mass within the aggregates as follows:

$$M(t) = \sum_{i=1}^N v_i c_i(t), \tag{13}$$

where  $M(t)$  is the oxygen mass within the agglomerate at time  $t$ , and  $c_i(t)$  is the concentration of the oxygen in  $i$ th agglomerate voxel at time  $t$ ,  $v_i$  is the volume of the ionomer in this voxel,



and  $N$  is the total number of the agglomerate voxels, excluding the voxels in the inter-agglomerate pores. The increasing rate of the oxygen mass in the agglomerates at time  $t$  was calculated from

$$r(t + \delta t / 2) = \frac{M(t + \delta t) - M(t)}{\delta t} \quad (14)$$

where  $\delta t$  is the time step. From the above discussions, the memory function can be calculated from

$$g(t) = \frac{r(t)}{\sum_{i=1}^N V_i} \quad (15)$$

where  $V_i$  is the volume of each agglomerate voxel.

Figure 5 shows the change of the calculated memory functions with time  $t$  for the two samples. They both drop sharply with time in the earlier stage, and decay exponentially in the later stage. It is evident that the exponential distribution function is inaccurate to describe these memory functions. The available model able to describe distribution functions with such a behaviour is the gamma distribution:

$$g(t) = \frac{\alpha (\alpha t)^{\kappa-1} \exp(-\alpha t)}{\Gamma(\kappa)}, \quad (16)$$

where  $\kappa$  and  $\alpha$  are parameters, and  $\Gamma(\kappa)$  is the gamma function. We use curve-fitting to find the two parameters for each sample.

Physically,  $\kappa$  controls the drop of the memory function with time in the earlier stage and  $\alpha$  in the later stage. Therefore, in curve fitting, we first estimated the values of the two parameters based on the head and tail of the simulated memory function. We then fine-tuned them, judged by visual inspection, until a best fitting was found. Figure 5 compares the best-fitting results with the memory functions directly calculated for the two samples. They agree reasonably well. The values of the best-fitting parameters are  $\kappa = 0.54$ ,  $\alpha = 0.024$  for the

idealised catalyst layer, and  $\kappa = 0.60$ ,  $\alpha = 0.054$  for the real catalyst layer. The two samples have comparable  $\kappa$ , but contrasting  $\alpha$  because the agglomerates in the idealised catalyst layer are much bigger and difficult for oxygen to move as shown in Figure 4.

#### 4. The proposed agglomerate model

The agglomerate model is linked to the memory function in Eq. (10). Substituting Eq. (16) into Eq.(10) gives

$$R_e = k_c c_m \int_0^\infty \frac{\alpha (\alpha \tau)^{\kappa-1}}{\Gamma(\kappa)} e^{-(\alpha+k_c)\tau} d\tau. \quad (17)$$

Rewriting the terms inside the integral so as to make it the density function of the gamma distribution, we derive an agglomerate model:

$$\begin{aligned} R_e &= \left( \frac{\alpha}{\alpha + k_c} \right)^\kappa k_c c_m \int_0^\infty \frac{(\alpha + k_c) [(\alpha + k_c) \tau]^{\kappa-1}}{\Gamma(\kappa)} e^{-(\alpha+k_c)\tau} d\tau \\ &= \left( \frac{\alpha}{\alpha + k_c} \right)^\kappa k_c c_m \\ &= E k_c c_m, \end{aligned} \quad (18)$$

where  $E = (1 + k_c / \alpha)^{-\kappa}$  is the effectiveness factor.

To demonstrate that the proposed model is indeed an improvement and able to reproduce what the spherical model can describe, we applied it to the example shown in Figure 2 for a spherical agglomerate with diameter of 300nm. Figure 6 compares the results calculated by the proposed model using parameters of  $\kappa = 0.48$  and  $\alpha = 7$  with the results of the spherical model under differential overpotentials. They agree well, indicating that the memory function we derived also applies to oxygen diffusion in spherical agglomerates. Although the proposed model is mathematically simpler, it is more general and the spherical agglomerate model can be viewed as its special case.

The parameter  $\kappa$  in the model is dimensionless and depends only on agglomerate geometry; it describes the decrease of the rate at which the oxygen moves from the inter-agglomerate pores to the agglomerates in the earlier stage. In contrast, the parameter  $\alpha$  has unit of  $\text{s}^{-1}$  and describes how easy the oxygen can move within the agglomerates in the later stage; it depends on both geometry and effective diffusion coefficient of the agglomerates. From the simulated results shown in Figure 5, the agglomerates in the idealised catalyst layer shown in Figure 2A are big and difficult for the oxygen to move, and it hence has a small  $\alpha$ . To elucidate how the two parameters affect the efficiency of the catalyst layer, Figure 7 shows the change of the effectiveness factor with overpotential under different combinations of the two parameters by fixing  $k_0$  at  $k_0 = 0.01$ .

## 5. Model verification

The memory function shown in Figure 5 is the probability that an oxygen molecule, which is initially on the agglomerate surface, enters and remains within the agglomerate at time  $t$  in the absence of any electrochemical reaction; it depends only on geometry of the agglomerate and its effective diffusion coefficient for oxygen to diffuse. When the oxygen molecule is also subjected to a reduction reaction at reduction rate of  $k_c$ , the probability that this oxygen molecule will be consumed by the reduction reaction at time  $t$  is  $g(t)e^{-k_c t}$ . To prove the agglomerate model derived from this analysis, we verified it against the average electrochemical reaction rates directly calculated from pore-scale simulations of oxygen diffusion and reaction in the two catalyst layers shown in Figure 2. The simulation procedure is similar to the above simulations for calculating the memory function, but with  $k_0 > 0$  and the overpotential varying from 0 V to 1.0 V. The values of other parameters used in the pore-scale simulations are given in Table 1. In each simulation, after the diffusion and reaction

were deemed to have reached steady state, the average electrochemical reaction rate was calculated from:

$$R_e = \frac{\sum_{i=1}^N v_i k_c c}{\sum_{i=1}^N V_i}, \quad (19)$$

where all the variables are the same as those defined in Eq.(13). We also use the effectiveness factor as follows to describe the decreased average electrochemical reaction rate:

$$R_e = E k_c c_m, \quad (20)$$

Equating Eq.(19) and Eq.(20) gives

$$E = \frac{\sum_{i=1}^N v_i c_i}{\sum_{i=1}^N V_i}. \quad (21)$$

Figure 8 compares the effectiveness factors directly calculated from the pore-scale simulations with that predicted from Eq. (18) with its two parameters estimated from the memory functions shown in Figure 5. Overall, they agree well. There are some discrepancies because the gamma distribution is an approximation, and it cannot perfectly match the simulated memory functions.

The significance of the proposed model is that its two parameters can be directly calculated from catalyst layer structures rather than by calibration. It can hence be used to help catalyst layer design. Although the agglomerate diameter in the spherical model is also a geometrical parameter, it is not a geometrical description of the agglomerates as it cannot be independently calculated from catalyst layer structures [15, 16]. This is why its value varies so widely in the literature ranging from 200 nm to 6000 nm [30, 31]. Physically, an agglomerate model should be able to link the agglomerate structures to catalyst layer performance, rather than just a mathematical bridge to fit curves. In this aspect, the proposed model is sound.

## 6. Impact of thin ionomer film

The above model is for agglomerates without ionomer coating. Real agglomerates are often coated by a thin ionomer film, and the dissolved oxygen needs to move through the thin film first before it can electrochemically react with electrons and protons within the agglomerate. Figure 9 shows an illustrative example of an agglomerate coated with a thin ionomer film  $\lambda$  nanometre thick. If we assumed that the dissolved oxygen concentration on the ionomer surface is in equilibrium with gaseous oxygen concentration and is a constant  $C^{eq}$ , and that the oxygen concentration at the interface between the ionomer film and the agglomerate surface is  $c_m$ , the local diffusive flux rate across the thin ionomer film can be estimated by

$$q = D_0 \frac{C^{eq} - c_m}{\lambda} \quad (22)$$

Therefore, in a unit volume of catalyst layer, the rate at which the oxygen moves through the ionomer film into the agglomerates is

$$Q = \iint_S q \cdot ds \quad (23)$$

where  $S$  is the interface between the ionomer film and the agglomerate surface. We can approximate Eq.(23) by

$$Q = S_0 D_0 \frac{C^{eq} - c_m}{\lambda} \quad (24)$$

where  $S_0 = \iint_S ds$  is the specific outer surface area of the agglomerate. From mass balance, at steady state it has  $Q = R_e$ . We hence have

$$S_0 D_0 \frac{C^{eq} - c_m}{\lambda} = E \cdot k_c \cdot c_m \quad (25)$$

Solving for  $c_m$  gives

$$R_e = E' k_c C^{eq},$$

$$E' = \left( \frac{1}{E} + \frac{\lambda k_c}{S_0 D_0} \right)^{-1}. \quad (26)$$

To test the accuracy of this approximation, Figure 10 compares the effectiveness factor directly calculated from pore-scale simulation with that predicted by Eq. (26) when the dimensionless thickness of the ionomer film is 2.

## 7. Discussion and Conclusions

The nanopores within the agglomerates in the catalyst layer of PEM fuel cell are difficult for oxygen to move and could become a limiting factor at high overpotential. How to describe such limitations is an important issue in fuel cell modelling. The spherical agglomerate model has been widely used to describe the decreased electrochemical reaction under this condition, but its inferiority is well understood as it assumed that the agglomerates in a catalyst layer are non-touched spheres with a single diameter. Given the inadequacy of the spherical agglomerate model, developing improved catalyst-layer models is required.

The advent and application of tomography in fuel cells has opened an avenue for improving catalyst layer modelling. For example, using FIB/SEM tomography one can obtain 3D structures of a catalyst layer at resolutions as fine as a few nanometres. By simulating oxygen diffusion and reaction in such 3D structures, we can directly calculate the average oxygen reaction rate at different conditions. The calculated average reduction rates can be saved in tabular forms as an input database to fuel cell modelling; this is the most accurate description of a catalyst layer. However, such a database could become extremely huge and time-consuming to numerically calculate when a variety of operating conditions need to be considered. Therefore, expressing this database by a simple analytical formula is practical useful, and this paper presents such a formula.

The formula was derived based on the relationship between the average electrochemical reaction rate and the probability that an oxygen molecule, which is initially on the agglomerate surfaces, enters and stays in the agglomerates at any time in the absence of any reactions. The distribution function of this probability can be directly calculated; we

calculated it for two catalyst layers with contrasting interior structures. We then proposed a formula to fit the calculated distribution functions, from which the formula for describing the average reduction rate was derived. The formula has two parameters, and they both can be estimated from the structures of the catalyst layers.

We verified the formula by first showing that it is indeed an improvement, and able to produce all the spherical model can describe. Hence, the spherical model can be viewed as one of special case of the proposed model. We then tested it against the average electrochemical reaction rates directly calculated from pore-scale simulations of oxygen diffusion and reaction in the two catalyst layers; the comparisons showed good agreements. The most significant improvement of the proposed model is that, for a given catalyst layer, its two parameters can be directly calculated rather than by calibration. Hence, the model can be used in design. This differs from the spherical agglomerate model in which the agglomerate diameter is a fitting parameter and cannot be calculated independently. Another advantage of the formula is that it can be used to simulate transient behaviour of PEM fuel cell [32], which the spherical model could not.

A primary test of the model against two very contrasting catalyst layers is promising, but its reliability needs further tests against more catalyst layers. This will become feasible as the use of tomography in catalyst layer characterization will produce more 3D images. It is expected that combining them with pore-scale modelling could considerably improve our understanding of the catalyst layer processes. This and our previous work made such an effort in attempts to get some insight into the physical and electrochemical processes occurring in the catalyst layer. The results can help us to test the reliability of the models that have been widely used in the literature and improve them if necessary. For simplicity, we limited to a simple scenario where there is no liquid water and the agglomerates are fully filled by

ionomer. Extending the model to more complicated scenarios is under development and the results will be presented in future publications.

### Acknowledgements

Part of this research was supported by the UK Technology Strategy Board (TSB Project No. TP/6/S/K3032H). We thank Dr. Hutzenlaub for sharing his FIB/SEM image.

### Appendix A

To eliminate the concentration  $c_{im}$  in Eq.(2), we apply the Laplace transform to the two concentrations as follows:

$$\begin{aligned}\overline{c_{im}} &= \int_0^{\infty} c_{im} \exp(-st) dt, \\ \overline{c_m} &= \int_0^{\infty} c_m \exp(-st) dt.\end{aligned}\quad (\text{A1})$$

After the Laplace transformation, Eq.(2) becomes

$$s\overline{c_{im}} + k_c \overline{c_{im}} = \alpha (\overline{c_m} - \overline{c_{im}}). \quad (\text{A2})$$

Solving for  $\overline{c_{im}}$  gives

$$\overline{c_{im}} = \frac{\alpha \overline{c_m}}{s + \alpha + \beta}. \quad (\text{A3})$$

Multiplying  $s$  to both sides of Eq.(A3) yields

$$s\overline{c_{im}} = \frac{s\alpha \overline{c_m}}{s + \alpha + \beta}. \quad (\text{A4})$$

Applying the inverse Laplace transform to (A4) leads to

$$\begin{aligned}\frac{\partial c_{im}}{\partial t} &= \int_0^t \frac{\partial c_m}{\partial \tau} g(t - \tau) \exp[-\beta(t - \tau)] d\tau, \\ c_{im} &= \int_0^t c_m g(t - \tau) \exp[-\beta(t - \tau)] d\tau.\end{aligned}\quad (\text{A5})$$

where  $g(t) = \alpha \exp(-\alpha t)$  is called memory function.



## References

- [1] S. Thiele, T. Furstenhaupt, D. Banham, T. Hutzenlaub, V. Birss, C. Ziegler, R. Zengerle, Multiscale tomography of nanoporous carbon-supported noble metal catalyst layers, *Journal of Power Sources*, 228 (2013) 185-192.
- [2] Y. Xiao, J.L. Yuan, B. Sunden, Process Based Large Scale Molecular Dynamic Simulation of a Fuel Cell Catalyst Layer, *J. Electrochem. Soc.*, 159 (2012) B251-B258.
- [3] Y. Wang, K.S. Chen, J. Mishler, S.C. Cho, X.C. Adroher, A review of polymer electrolyte membrane fuel cells: Technology, applications, and needs on fundamental research, *Appl. Energy*, 88 (2011) 981-1007.
- [4] S. Kamarajugadda, S. Mazumder, Numerical investigation of the effect of cathode catalyst layer structure and composition on polymer electrolyte membrane fuel cell performance, *Journal of Power Sources*, 183 (2008) 629-642.
- [5] S. Kamarajugadda, S. Mazumder, Generalized flooded agglomerate model for the cathode catalyst layer of a polymer electrolyte membrane fuel cell, *Journal of Power Sources*, 208 (2012) 328-339.
- [6] S. Thiele, R. Zengerle, C. Ziegler, Nano-morphology of a polymer electrolyte fuel cell catalyst layer-imaging, reconstruction and analysis, *Nano Research*, 4 (2011) 849-860.
- [7] W.K. Epting, J. Gelb, S. Litster, Resolving the Three-Dimensional Microstructure of Polymer Electrolyte Fuel Cell Electrodes using Nanometer-Scale X-ray Computed Tomography, *Adv. Funct. Mater.*, 22 (2012) 555-560.
- [8] D. Harvey, J.G. Pharoah, K. Karan, A comparison of different approaches to modelling the PEMFC catalyst layer, *Journal of Power Sources*, 179 (2008) 209-219.
- [9] T. Suzuki, K. Kudo, Y. Morimoto, Model for investigation of oxygen transport limitation in a polymer electrolyte fuel cell, *Journal of Power Sources*, 222 (2013) 379-389.
- [10] F.C. Cetinbas, S.G. Advani, A.K. Prasad, Three dimensional proton exchange membrane fuel cell cathode model using a modified agglomerate approach based on discrete catalyst particles, *Journal of Power Sources*, 250 (2014) 110-119.
- [11] N.A. Siddique, F.Q. Liu, Process based reconstruction and simulation of a three-dimensional fuel cell catalyst layer, *Electrochim. Acta*, 55 (2010) 5357-5366.
- [12] E.W. Thiele, Relation between catalytic activity and size of particle, *Industrial and Engineering Chemistry*, 31 (1939) 916-920.
- [13] F.Q. Liu, B.L. Yi, D.M. Xing, J.R. Yu, Z.J. Hou, Y.Z. Fu, Development of novel self-humidifying composite membranes for fuel cells, *J. Power Sources*, 124 (2003) 81-89.
- [14] C. Ziegler, S. Thiele, R. Zengerle, Direct three-dimensional reconstruction of a nanoporous catalyst layer for a polymer electrolyte fuel cell, *Journal of Power Sources*, 196 (2011) 2094-2097.
- [15] X. Zhang, H. Ostadi, K. Jiang, R. Chen, Reliability of the spherical agglomerate models for catalyst layer in polymer electrolyte membrane fuel cells, *Electrochim. Acta*, 133 (2014) 475-483.
- [16] W.K. Epting, S. Litster, Effects of an agglomerate size distribution on the PEFC agglomerate model, *Int. J. Hydrog. Energy*, 37 (2012) 8505-8511.
- [17] M. El Hannach, T. Soboleva, K. Malek, A.A. Franco, M. Prat, J. Pauchet, S. Holdcroft, Characterization of pore network structure in catalyst layers of polymer electrolyte fuel cells, *Journal of Power Sources*, 247 (2014) 322-326.
- [18] K.J. Lange, P.C. Sui, N. Djilali, Pore Scale Simulation of Transport and Electrochemical Reactions in Reconstructed PEMFC Catalyst Layers, *J. Electrochem. Soc.*, 157 (2010) B1434-B1442.
- [19] S. Zils, M. Timpel, T. Arlt, A. Wolz, I. Manke, C. Roth, 3D Visualisation of PEMFC Electrode Structures Using FIB Nanotomography, *Fuel Cells*, 10 (2010) 966-972.

- [20] T. Hutzenlaub, J. Becker, R. Zengerle, S. Thiele, Modelling the water distribution within a hydrophilic and hydrophobic 3D reconstructed cathode catalyst layer of a proton exchange membrane fuel cell, *Journal of Power Sources*, 227 (2013) 260-266.
- [21] G.R. Molaeimanesh, M.H. Akbari, A three-dimensional pore-scale model of the cathode electrode in polymer-electrolyte membrane fuel cell by lattice Boltzmann method, *Journal of Power Sources*, 258 (2014) 89-97.
- [22] K.J. Lange, P.C. Sui, N. Djilali, Determination of effective transport properties in a PEMFC catalyst layer using different reconstruction algorithms, *Journal of Power Sources*, 208 (2012) 354-365.
- [23] K.J. Lange, H. Carlsson, I. Stewart, P.C. Sui, R. Herring, N. Djilali, PEM fuel cell CL characterization using a standalone FIB and SEM: Experiments and simulation, *Electrochim. Acta*, 85 (2012) 322-331.
- [24] Q.P. Wang, D.T. Song, T. Navessin, S. Holdcroft, Z.S. Liu, A mathematical model and optimization of the cathode catalyst layer structure in PEM fuel cells, *Electrochim. Acta*, 50 (2004) 725-730.
- [25] W. Sun, B.A. Peppley, K. Karan, An improved two-dimensional agglomerate cathode model to study the influence of catalyst layer structural parameters, *Electrochim. Acta*, 50 (2005) 3359-3374.
- [26] V. Cvetkovic, A general memory function for modeling mass transfer in groundwater transport, *Water Resources Research*, 48 (2012) 12.
- [27] R. Haggerty, S.M. Gorelick, Multiple-rate mass-transfer for modelling diffusion and surface-reaction in media with pore-scale heterogeneity *Water Resources Research*, 31 (1995) 2383-2400.
- [28] X.X. Zhang, X.B. Qi, D.M. Qiao, Change in macroscopic concentration at the interface between different materials: Continuous or discontinuous, *Water Resources Research*, 46 (2010) 12.
- [29] X.X. Zhang, X.B. Qi, D.M. Qiao, Change in macroscopic concentration at the interface between different materials: Continuous or discontinuous, *Water Resour. Res.*, 46 (2010).
- [30] A.A. Shah, G.S. Kim, W. Gervais, A. Young, K. Promislow, J. Li, S. Ye, The effects of water and microstructure on the performance of polymer electrolyte fuel cells, *Journal of Power Sources*, 160 (2006) 1251-1268.
- [31] N.P. Siegel, M.W. Ellis, D.J. Nelson, M.R. von Spakovsky, Single domain PEMFC model based on agglomerate catalyst geometry, *Journal of Power Sources*, 115 (2003) 81-89.
- [32] S.M. Chang, H.S. Chu, Transient behavior of a PEMFC, *Journal of Power Sources*, 161 (2006) 1161-1168.

**Fig. 1** An illustration of cathode catalyst layer where oxygen diffusion and reaction take place in the black agglomerates containing nanopores. The yellow spots are the catalysts (not in scale). Gaseous oxygen concentration in the inter-agglomerate pores is  $C$ ; oxygen dissolves in the ionomer on the agglomerate surfaces, and the dissolved oxygen concentration is  $c_m$ . The representative oxygen concentration inside the agglomerates is  $c_{im}$ . The difference between  $c_m$  and  $c_{im}$  drives the oxygen diffusing into the agglomerates at a rate of  $R_0$ .

**Fig. 2** Comparison between the effectiveness factors calculated by the spherical agglomerate model and the simple model under different overpotentials.

**Fig. 3** The two catalyst layers simulated in this work: (A) An idealised catalyst layer made by non-overlapped spheres; (B) a real catalyst layer acquired using FIB/SEM tomography.

**Fig. 4** Snapshots of the simulated concentration distributions at  $t' = 15$  in the idealised catalyst layer (A), and in the real catalyst layer (B). The normalised concentration changes from 1 (red) to 0.001 (blue).

**Fig. 5** Change of the memory functions with time calculated from pore-scale simulations of oxygen diffusion in the two samples shown in Figure 3. (A) The real catalyst layer, (B) the idealised catalyst layer.

**Fig. 6** Comparison of the effectiveness factors calculated by the spherical model and the proposed model, showing that the former can be viewed as special case of the latter.

**Fig. 7** Impact of different combinations of the two model parameters on the effectiveness factors calculated using  $k_0 = 0.01$ . (A) Fix  $\kappa$  at 0.48 and change  $\alpha$ , (B) and fix  $\alpha$  at 7 and change  $\kappa$ .

**Fig. 8** Comparison between the effectiveness factors directly calculated from pore-scale simulations of oxygen diffusion and reaction in the two samples shown in Figure 3 with that predicted from the proposed model with its two parameters estimated from Figure 5. (A) Comparison for the idealised catalyst layer; (B) comparison for the real catalyst layer acquired using FIB/SEM.

**Fig. 9** A schematic illustration of oxygen diffusion from inter-agglomerate pores into the agglomerate through a thin ionomer film  $\lambda$  nanometres thick. Blue is air, red is ionomer film and green is agglomerate.

**Fig. 10** Comparison between the effectiveness factors directly calculated from pore-scale simulations (symbols) with that predicted from the approximate model (solid line) when the agglomerate is coated by a thin ionomer film with a dimensionless thickness of 2.

ACCEPTED MANUSCRIPT

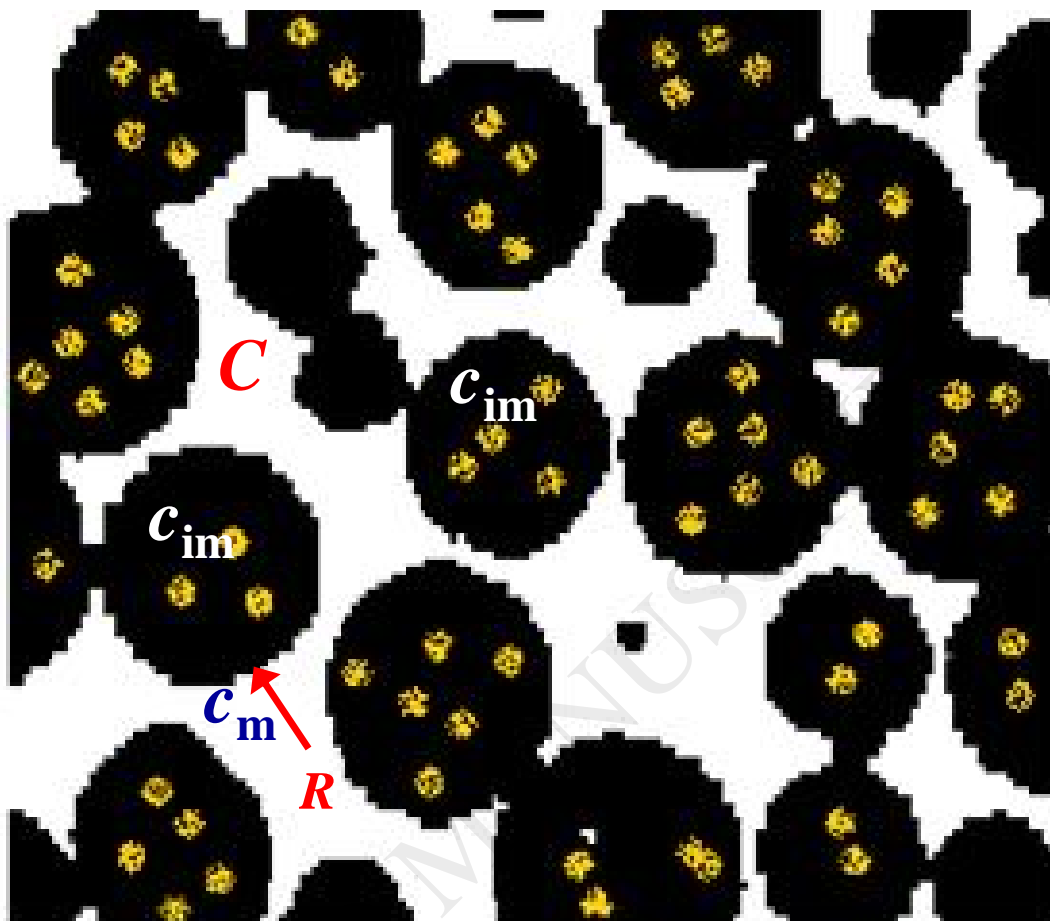


**Fig. 1** An illustration of cathode catalyst layer where oxygen diffusion and reaction take place in the black agglomerates containing nanopores. The yellow spots are the catalysts (not in scale). Gaseous oxygen concentration in the inter-agglomerate pores is  $C$ ; oxygen dissolves in the ionomer on the agglomerate surfaces, and the dissolved oxygen concentration is  $c_m$ . The representative oxygen concentration inside the agglomerates is  $c_{im}$ . The difference between  $c_m$  and  $c_{im}$  drives the oxygen diffusing into the agglomerates at a rate of  $R_0$ .

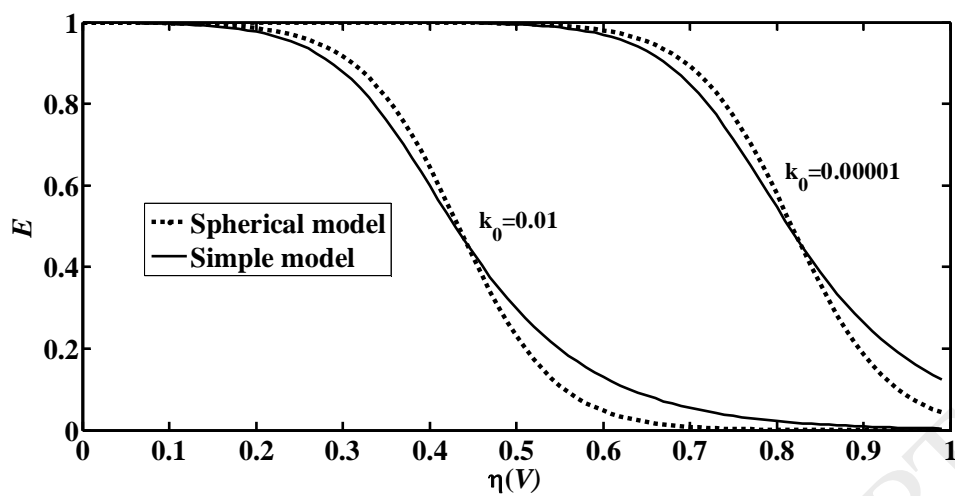
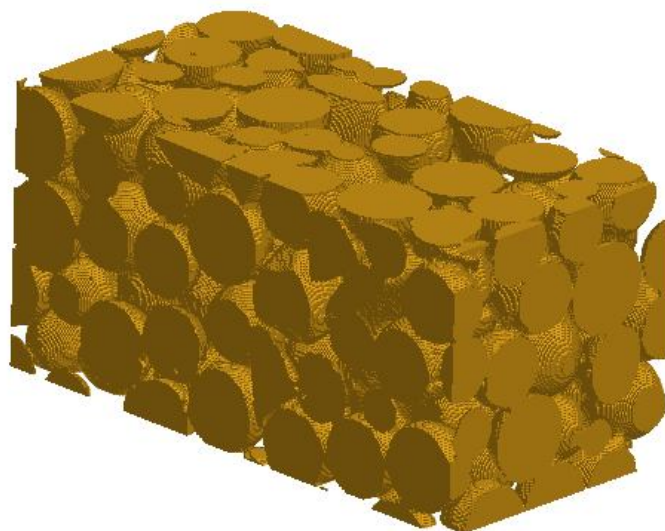
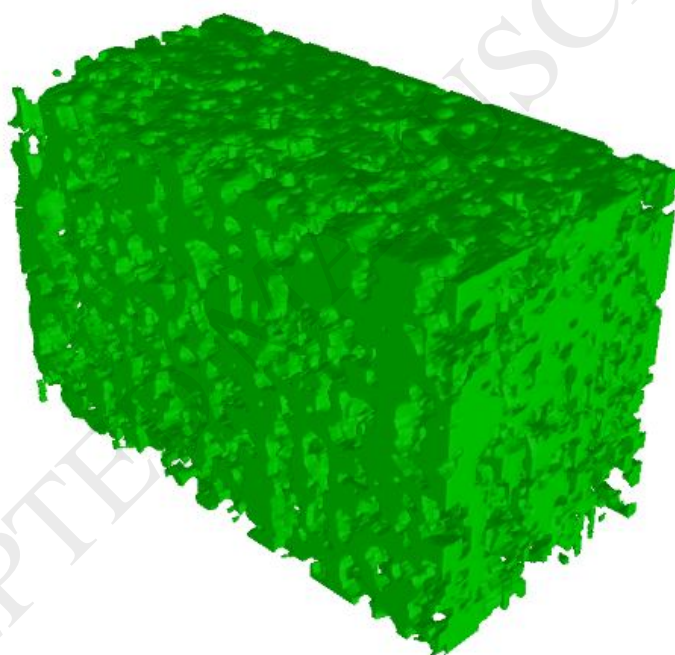


**Fig. 2** Comparison between the effectiveness factors calculated by the spherical agglomerate model and the simple model under different overpotentials.



(A)



(B)

**Fig. 3** The two catalyst layers simulated in this work: (A) An idealised catalyst layer made by non-overlapped spheres; (B) a real catalyst layer acquired using FIB/SEM tomography.

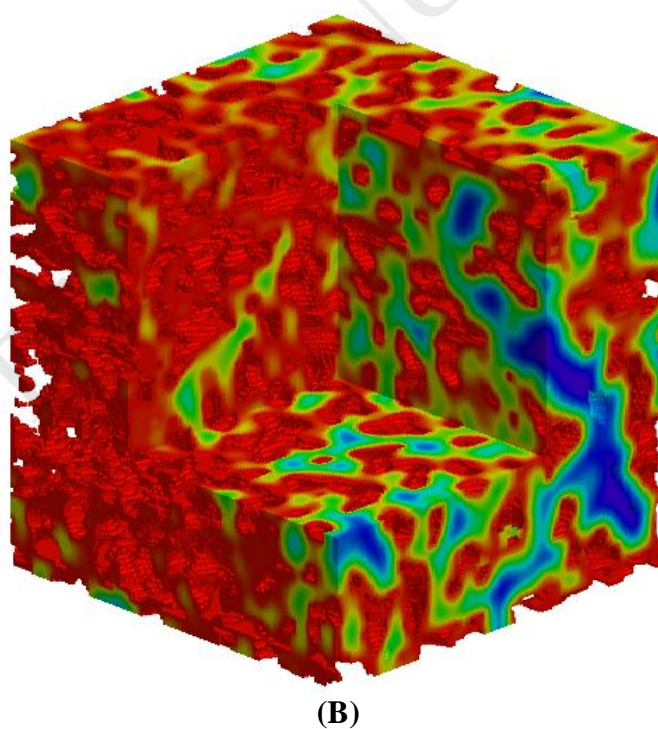
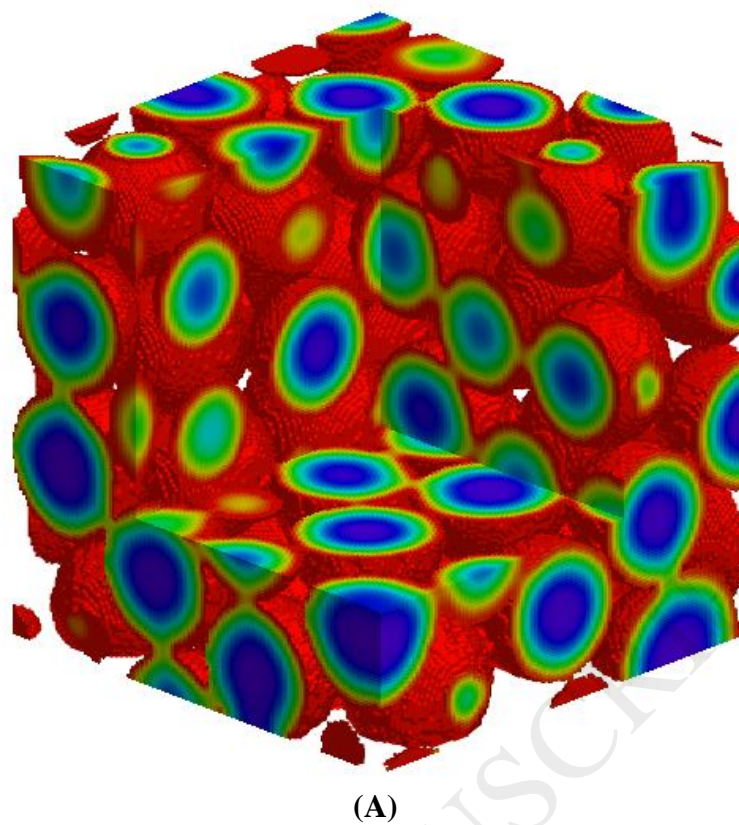


**Fig. 4** Snapshots of the simulated concentration distributions at  $t' = 15$  in the idealised catalyst layer (A), and in the real catalyst layer (B). The normalised concentration changes from 1 (red) to 0.001 (blue).



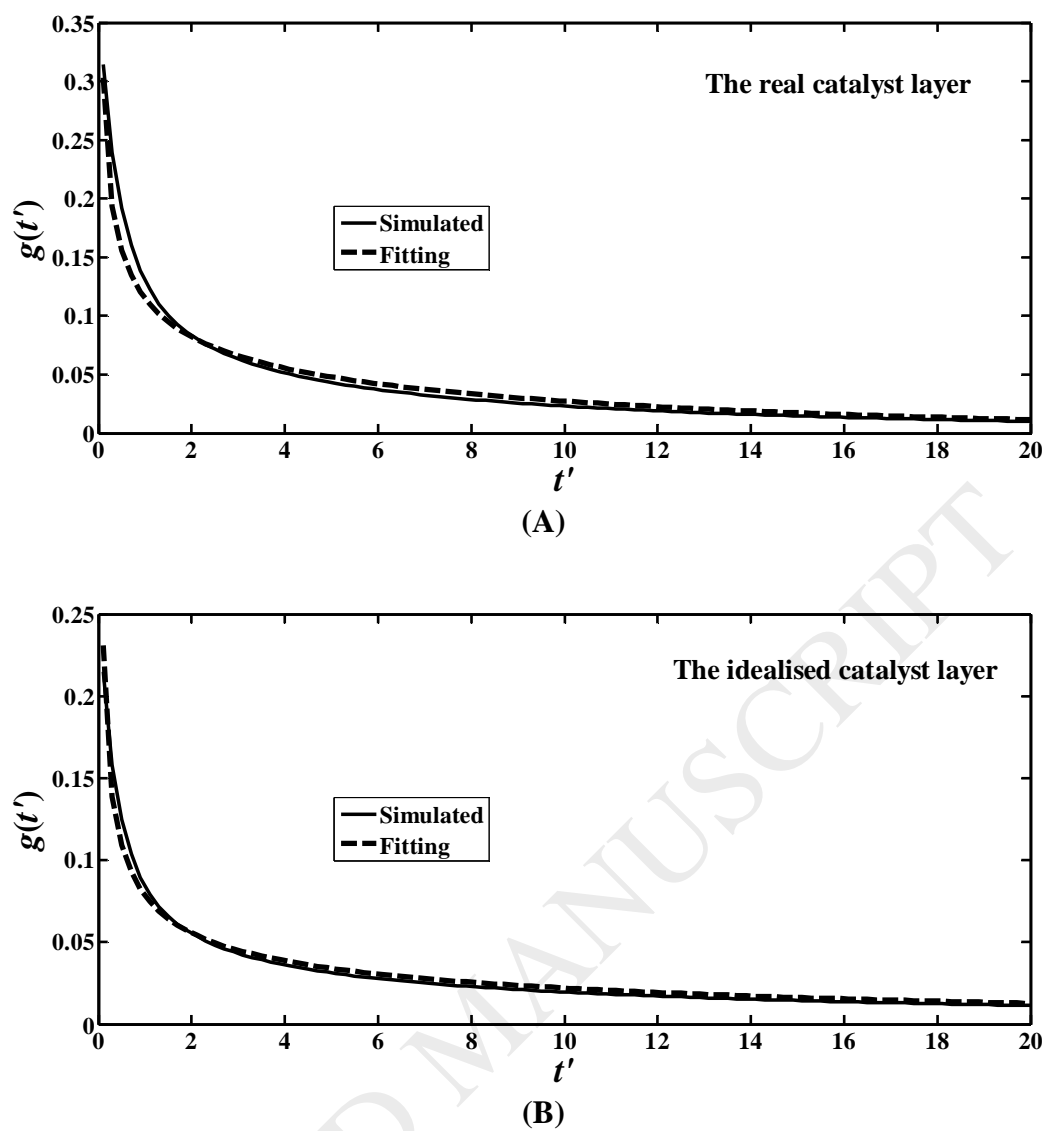


**Fig. 5** Change of the memory functions with time calculated from pore-scale simulations of oxygen diffusion in the two samples shown in Figure 3. (A) The real catalyst layer, (B) the idealised catalyst layer.

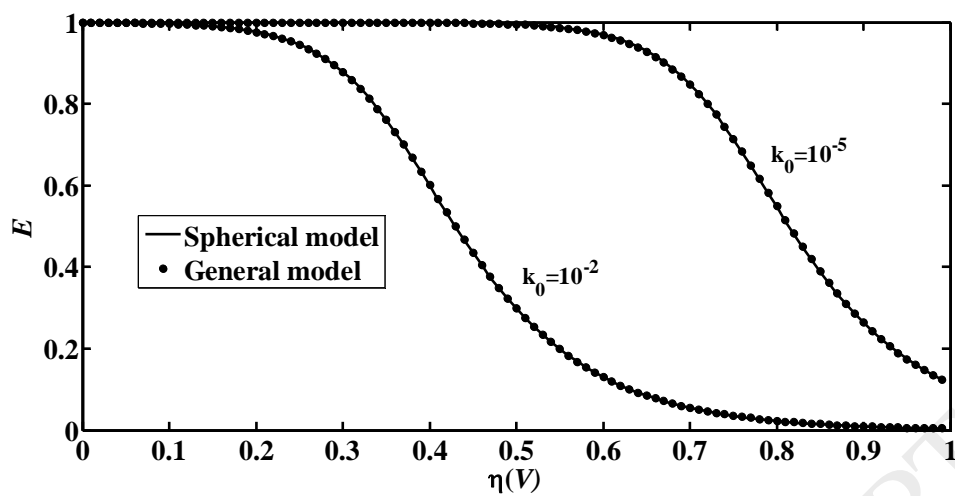


**Fig. 6** Comparison of the effectiveness factors calculated by the spherical model and the proposed model, showing that the former can be viewed as special case of the latter.

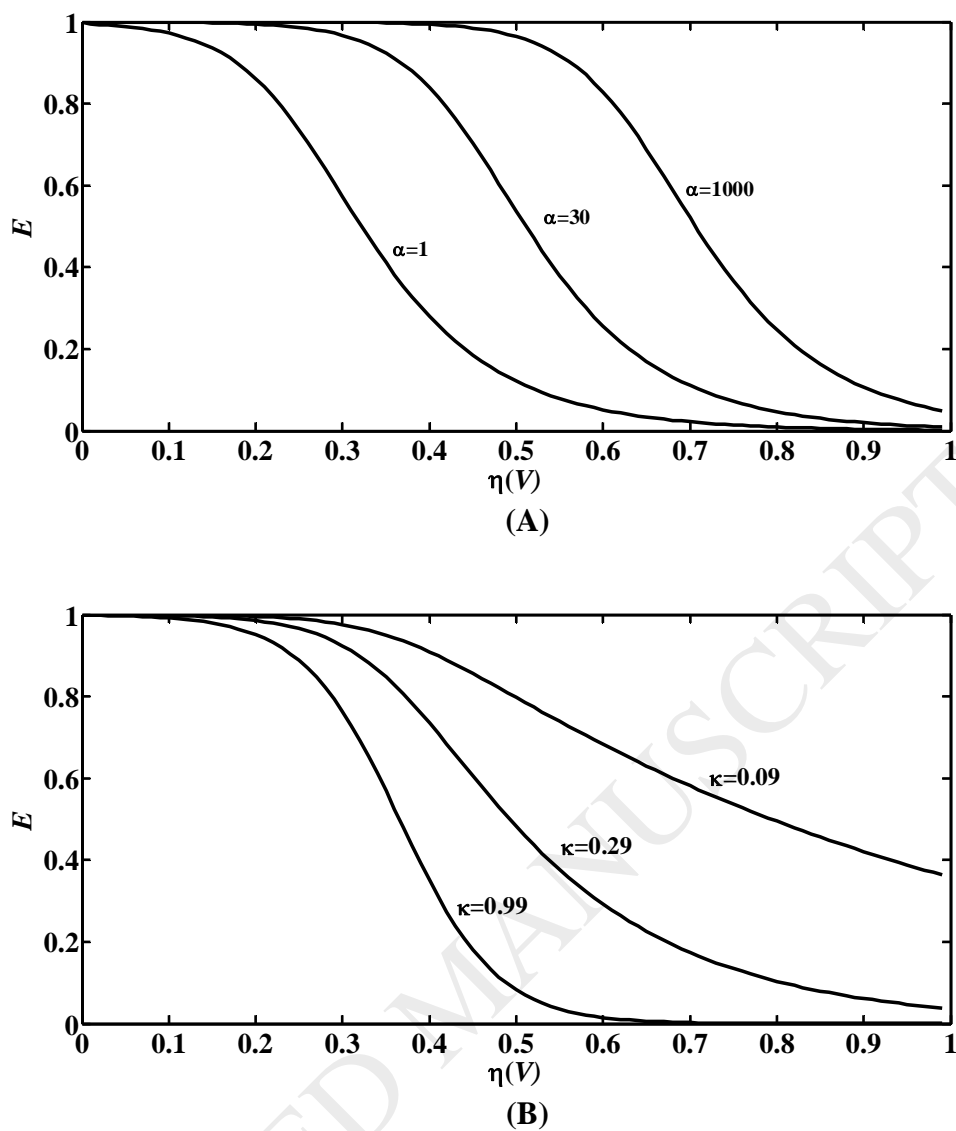


**Fig. 7** Impact of different combinations of the two model parameters on the effectiveness factors calculated using  $k_0=0.01$ . (A) Fix  $\kappa$  at 0.48 and change  $\alpha$ , (B) and fix  $\alpha$  at 7 and change  $\kappa$ .

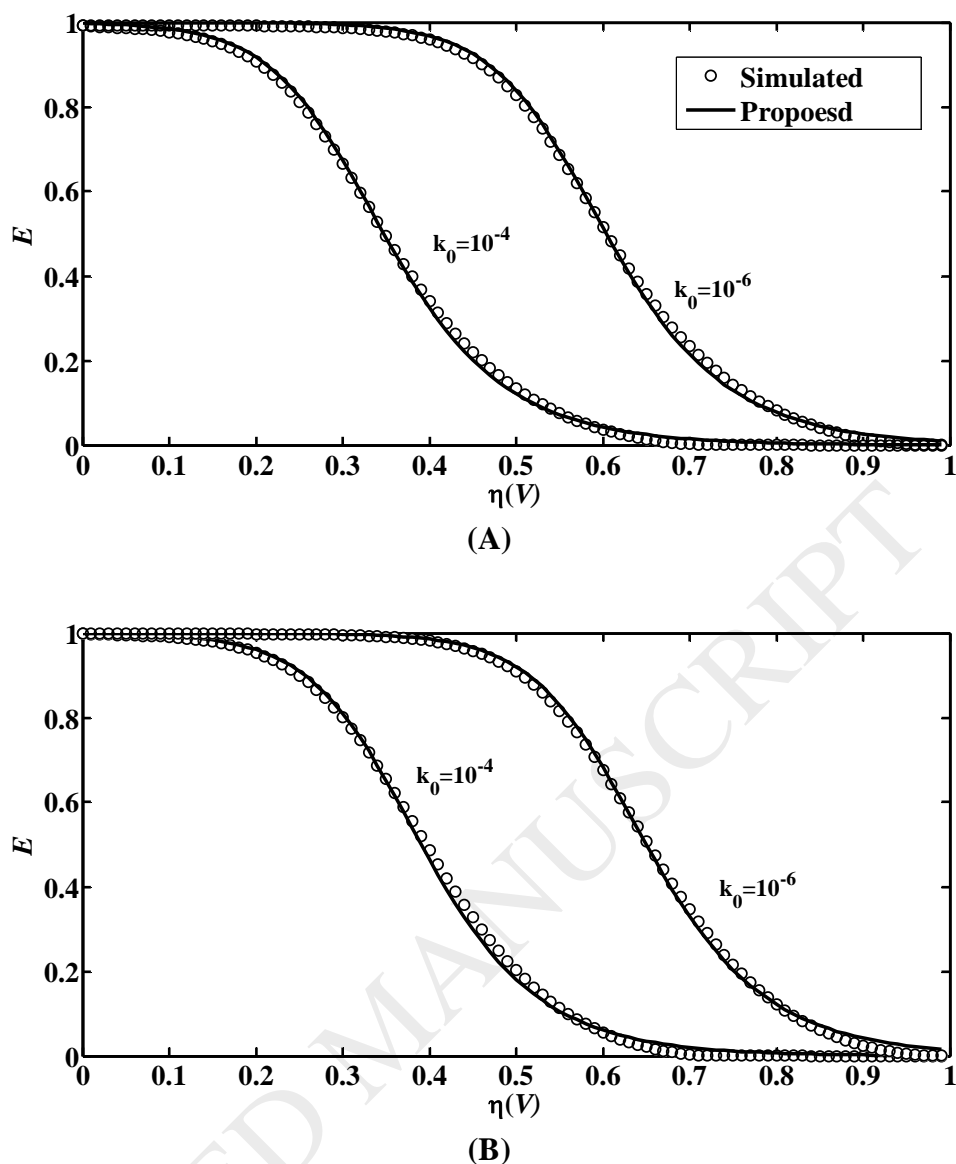


**Fig. 8** Comparison between the effectiveness factors directly calculated from pore-scale simulations of oxygen diffusion and reaction in the two samples shown in Figure 3 with that predicted from the proposed model with its two parameters estimated from Figure 5. (A) Comparison for the idealised catalyst layer; (B) comparison for the real catalyst layer acquired using FIB/SEM.

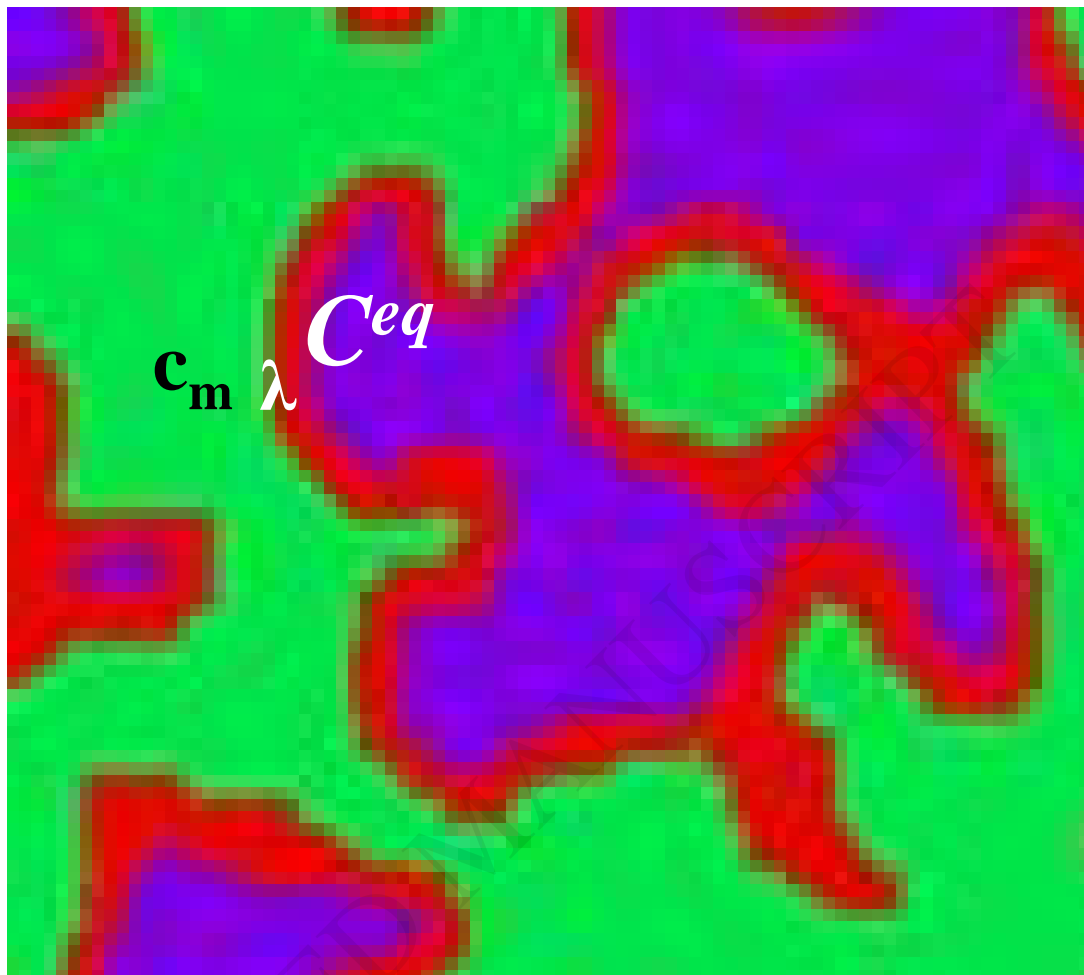


**Fig. 9** A schematic illustration of oxygen diffusion from the inter-agglomerate pores into the agglomerate through a thin ionomer film  $\lambda$  nanometres thick. Blue is air, red is ionomer film and green is agglomerate.

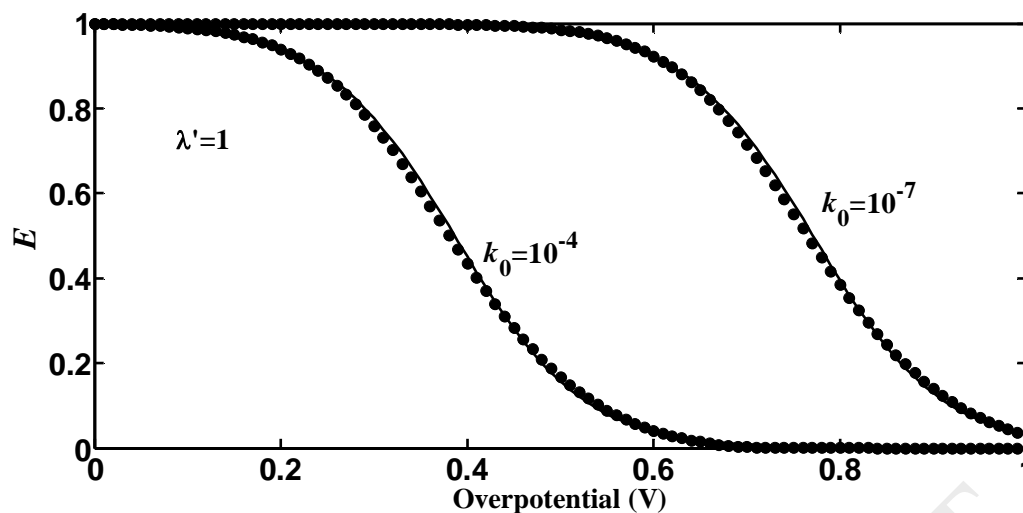


**Fig. 10** Comparison between the effectiveness factors directly calculated from pore-scale simulations (symbols) with that predicted from the approximate model (solid line) when the agglomerate is coated by a thin ionomer film with a dimensionless thickness of 2.

**Table 1** Physical properties and constant parameters used in the simulations

Parameter	Value
Cell temperature (K)	323.15
Volumetric fraction of ionomer (%)	30
Oxygen diffusion coefficient in ionomer ( $\text{m}^2\text{s}^{-1}$ )	$8.45 \times 10^{-10}$
Oxygen reference concentration ( $\text{mol m}^{-3}$ )	0.85
Cathode transfer coefficient	0.5
Electrochemically active surface area ( $\text{m}^2\text{m}^{-3}$ )	$1.04 \times 10^7 \sim 1.04 \times 10^8$
Faraday constant ( $\text{C mol}^{-1}$ )	96485
Gas constant ( $\text{J mol}^{-1}\text{K}^{-1}$ )	8.314